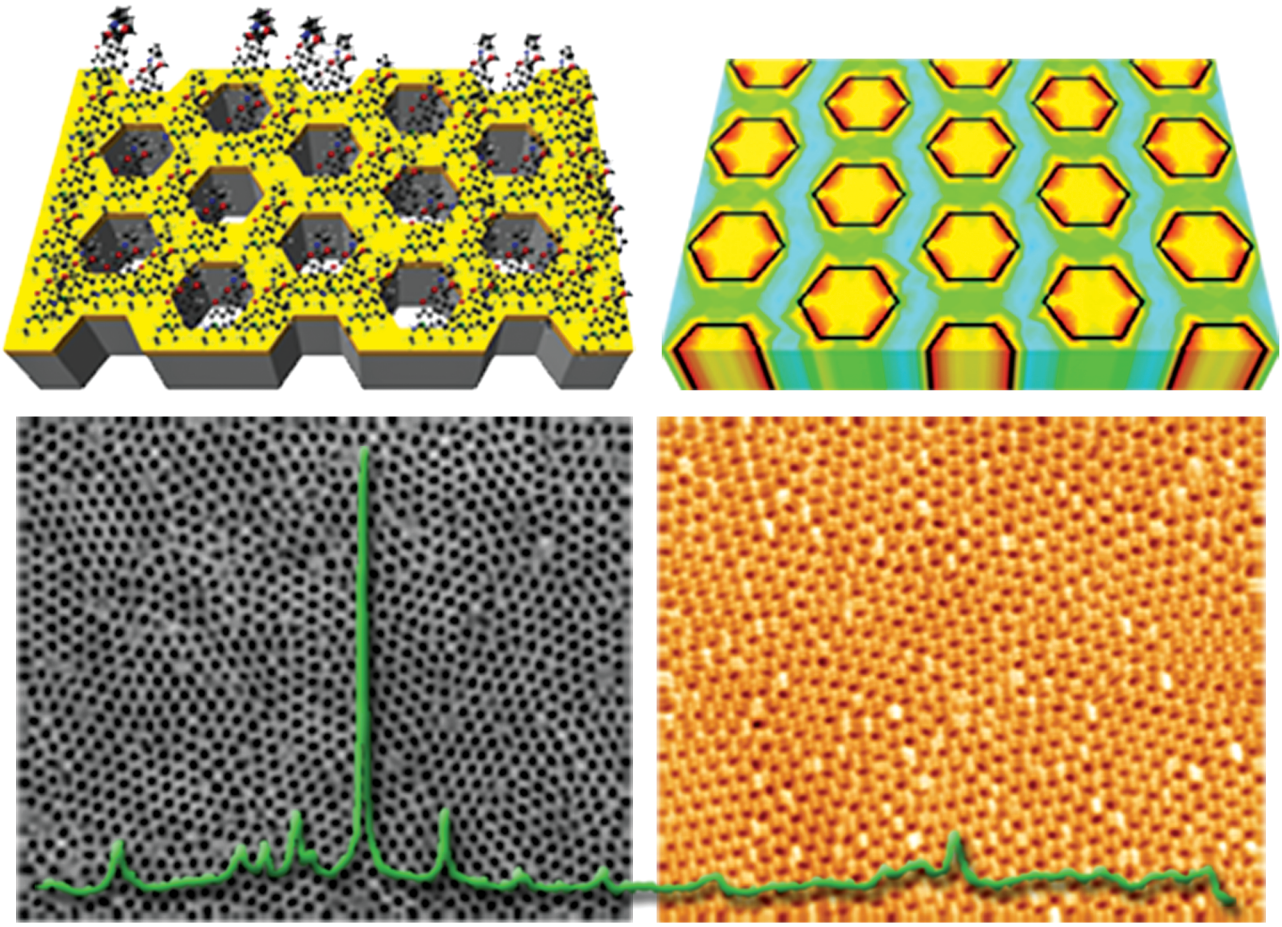

Showcasing research of the Nanostructure Division at the Italian Institute of Technology, Genoa, Italy, which is involved in the research of single molecule detection using SERS, TERS and SENSe techniques under Professor Enzo Di Fabrizio.

Title: Fabrication of large-area ordered and reproducible nanostructures for SERS biosensor application

Anodic porous alumina template based SERS substrates with varying pore size and wall thickness were fabricated. Various molecules (cresyl violet, rhodamine 6G and GFP protein) were deposited on honey-comb nano-patterned SERS substrates using a chemisorption technique. Theoretical simulation shows excellent agreement with experiment findings.

As featured in:

See Gobind Das *et al.*, *Analyst*, 2012, **137**, 1785–1792.

RSC Publishing

www.rsc.org/analyst

Registered Charity Number 207890

Analyst

Dynamic Article Links

Cite this: *Analyst*, 2012, **137**, 1785

www.rsc.org/analyst

PAPER

Fabrication of large-area ordered and reproducible nanostructures for SERS biosensor application†

Gobind Das,* Niranjan Patra, Anisha Gopalakrishnan, Remo Proietti Zaccaria, Andrea Toma, Sanjay Thorat, Enzo Di Fabrizio, Alberto Diaspro and Marco Salerno

Received 27th October 2011, Accepted 13th January 2012
DOI: 10.1039/c2an16022f

We propose a large-area SERS device with efficient fluorescence quenching capability. The substrate is based on anodic porous alumina templates with various pore size and wall thickness as small as 15 and 36 nm, respectively. The nano-patterned SERS substrate, with excellent control and reproducibility of plasmon-polaritons generation, shows very efficient enhanced Raman signal in the presence of intrinsically fluorescent molecules such as cresyl violet, rhodamine, and green fluorescent protein. This work demonstrates that, when the nanostructures are properly designed and fabricated, Raman and fluorescence spectroscopy can be used in combination in order to obtain complementary molecular informations. Theoretical simulation shows excellent agreement with the experimental findings. The enhancement factor is found to be 10^3–10^4, with respect to flat gold surface when the molecules are supposed to be closely packed, with considerable fluorescence suppression, showing a promising disposable biosensor.

Introduction

Surface-enhanced Raman scattering (SERS) is an analytical technique extensively used in chemistry, biology and forensic science, due to its excellent sensitivity for molecular vibrations.[1–3] The overall enhancement of the Raman signal occurs in SERS because of the combined (dominating) electromagnetic effect, due to resonant excitation of localized surface plasmons (LSPs) in noble metal surface structures, and a (smaller) chemical effect, due to the appearance of charge transfer bands in the electronic spectrum of the dye molecules, arising from the presence of the adjacent metal levels.[4] Giant electromagnetic fields can be generated when nano-structured features on metal (*e.g.*: Ag, Au, Cu) substrates are excited by light, causing LSP generation.[5,6] As it is well known that the intensity of LSP resonance strictly depends on the size, shape, inter-particle gap and dielectric environment of the material, these parameters should be chosen carefully, keeping in mind the reproducibility of the SERS substrate. The pattern of metal nanostructures, obtained so far on the substrate, was either produced by solvent-cast deposition of colloidal particles[7,8] or by lithographic techniques such as electron beam lithography, allowing for the fabrication of highly regular patterns.[9,10] The colloidal particle substrate can cover a large surface area but the drawback is a random deposition of the particles, resulting in a disordered distribution of hot-spots. On the other hand, lithographically made substrates can provide excellent control on density and position of the hot-spots, but have several limitations such as high cost, long production time, and small patterned area, which is typically in mm^2 range.[11]

In fact, the critical concerns to resolve which hamper the SERS applications are: (1) the absence of significant average-area SERS enhancement for large area, and (2) the existence of a sparse distribution of the hot-spots. Nanosphere lithography,[12–15] employed to fabricate the SERS device, is a technique at present which overcomes the above limitation as it can be fabricated on the large area. In this work, a new technique is proposed based on a gold-coated anodic porous alumina (APA) template as a convenient SERS substrate with large-area patterning. The porosity, wall thickness, pore size, *etc.* of the APA substrate can be modulated by proper fabrication parameters such as the electrolytic potential, electrolyte solution, etching time, *etc.*

In the present work, APA substrates, having hexagonal periodicity,[16,17] were fabricated following different protocols,[18–20] which allowed us to obtain different pore diameters and pore wall thicknesses. The fabricated APA substrates were used as a templates for the preparation of nano-patterned gold surfaces, obtained by gold film deposition of ~25 nm thickness covering the APA features. The novelty of our SERS substrate fabrication is to achieve reproducible SERS substrates with the wall thickness and pore diameter down to 15 and 36 nm, respectively, by varying the acid in the aqueous electrolyte and the anodization voltage. It is noticeable that they show very efficient SERS signals in the presence of intrinsically fluorescent molecules. The substrate surface morphology was characterized by both atomic force microscopy (AFM) and scanning electron microscopy

Italian Institute of Technology, via Morego 30, I-16163 Genoa, Italy. E-mail: gobind.das@iit.it; Fax: +39-010-720321; Tel: +39-010-71781217
† Electronic supplementary information (ESI) available. See DOI: 10.1039/c2an16022f

(SEM), and the performance as a SERS substrate was tested with three different substances, namely cresyl violet (CV), rhodamine 6G (Rd6G) and green fluorescence protein mut2 (GFPmut2). These substances fluoresce at distinct wavelengths in the visible spectrum from the red to violet region. Though, it is well known that a metal surface acts as a fluorescence quenching substrate,[21] it is the first time that the same SERS substrate has been employed for molecules having fluorescence in such a wide spectral region. Therefore, gold-coated APA templates ('AuAPA') were demonstrated to be an effective universal SERS substrate, accessible to understand the chemical vibrations of several types of molecules under investigation. In addition, simulations of the electric field distribution from linearly polarized light impinging on the SERS substrates were also carried out using a dedicated software package, which confirmed the excellent substrate performance.

Experimental

Fabrication of the APA templates

The home-built APA substrate was prepared at +7 °C external bath temperature with electrolyte stirring, by controlled modification of a 250 μm thick foil of ultrapure (99.999%) aluminium as the anode, in the same open electrochemical cell configuration as in previous experiments.[22] The cathode was made of a platinum foil of similar purity and geometry. First, the aluminium foil was electropolished in a 1 : 5 v/v aqueous solution of $HClO_4 : C_2H_5OH$ mixture, run for 5 min at a constant current density $J_{EP} \approx 170$ mA cm^{-2}. Then, anodization was carried out in aqueous solutions of different acids (*i.e.* phosphoric, oxalic and sulfuric acid) in order to obtain the different pore diameters. In all cases, the anodization regime was potentiostatic and relied on a two-step process. Firstly, the anodization step was performed for a short time period (~1 h), which allowed us to obtain a pre-patterning of the aluminium surface. After this step, the APA layer was dissolved by chemical wet etching in a 3 : 1 v/v aqueous solution of concentrated $H_3PO_4 : H_2CrO_4$ mixture at ~60 °C for ~40 min. The second anodization was carried out overnight for ~12 h.

For the large-pore APA (substrate 'APA1') anodization was carried out in 0.4 M H_3PO_4 at ~130 V; for the medium sized pore APA ('APA2') it was carried out in 0.3 M $H_2C_2O_2$ at 40 V; and for the small-pore APA ('APA3') it was carried out in 0.3 M H_2SO_4 at 25 V.

All the anodized APAs underwent pore cleaning and widening in 10 wt% H_3PO_4 at 35 °C for 45 min. Finally the APA substrates were repeatedly washed with de-ionized (DI) water, sonicated in DI water for ~1 min, and then the samples were blown dry with N_2. The depth of the pores is found to be 50–80 μm which is also the thickness of the APA membrane.

An approximate sketch of the APA substrate geometry is shown in Fig. 1a, where the pore diameter d, the cell dimension D, and the wall thickness w, are indicated.

Preparation of the SERS substrates

In order to provide the surfaces with plasmon functionality, gold was thermally evaporated from a tungsten boat onto the APA substrates ('APA1', 'APA2' and 'APA3'), starting the deposition

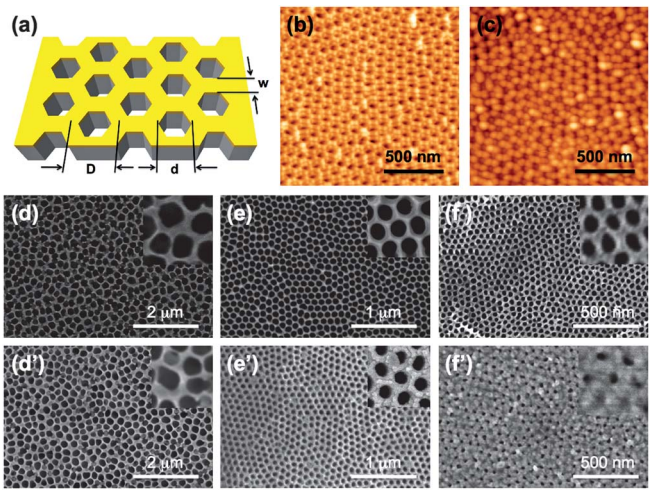

Fig. 1 (a) Ideal APA honey-comb structure; (b) and (c) representative AFM images of APA2 substrates before and after gold coating, respectively; (d–f) SEM images of APA1, APA2 and APA3 substrates, respectively; (d′–f′) represent the same APA substrates after gold coating. In the insets a local additional magnification of 3× allows to better see details of the porous structures.

at a base chamber pressure of 2.0×10^{-6} mbar and proceeding at 0.5 Å s^{-1} until a final total thickness of ~25 nm was reached. During deposition the sample holder was rotated at 1 RPM in order to improve the uniformity and the morphological quality of the gold layer. A process flow diagram of SERS substrate fabrication on the APA template was illustrated in Fig. S1† (Supplementary Info: section 1). The cross-section SEM measurements indicate that the gold grains are present up to 100–150 nm from the surface, shown in Fig. S2† (Supplementary Info: section 2).

The substance of interest was deposited over resulting gold-coated APA substrates (termed 'AuAPA1', 'AuAPA2' and 'AuAPA3', respectively) using a chemisorption technique. In this process, the substrate was dipped into a solution containing the molecule of interest. After incubation, each substrate was removed from the solution, gently rinsed to remove excess molecules not attached directly to the metal surface. Thereafter, the samples were dried in N_2 flow, and finally stored in a desiccator before SERS measurements. Various fluorescent dyes were tested for SERS probes, namely CV, Rd6G and GFPmut2 with the concentration in the order of 10^{-6} M. These molecules have an absorption band in the range of the optical region from 480–585 nm.

Characterization techniques

AFM measurements were performed on the APA substrates with an MFP-3D instrument (Asylum Research, USA) operating in air in tapping mode by means of NSG10 probes (NT-MDT, Russia), consisting of gold-coated silicon cantilevers with standard tip shapes (nominal apex diameter 20 nm) and nominal spring constant and resonance frequency of $k \approx 12$ N m^{-1} and $f_0 \approx 240$ kHz, respectively. All the APA substrates were measured in the AFM both before and after gold deposition, which resulted in similar instances of pore diameter decreasing

and corresponding pore wall thickening. In Fig. 1(b–c), only the case for APA2 before and after gold deposition is shown.

SEM measurements (JSM-7500FA, Jeol, Japan) were also performed on the APA substrates, keeping the 15 kV acceleration voltage for the primary electron beam and collecting the topographic signal from the secondary electrons. For imaging of the specimens before gold coating the SEM was operated in low vacuum conditions (70–120 Pa residual chamber pressure) in order to prevent major static charging effects due to the impinging electron beam. Since the SEM images are not affected by AFM tip convolution effects, which make the pore wall appear thicker than it is in reality, image analysis to determine the pore and wall size was carried out on the SEM images only. To this goal, dedicated routines available in the Igor Pro 6.0 software program (Wavemetrics, USA) have been used, which allowed us to extract the data reported in Table 1. All the reported data are written as mean values ± standard deviation.

The mean wall thickness, w is given by

$$w = D - d \tag{1}$$

The surface coverage of the pores, P, is

$$P = \frac{N_{\text{pore}} \times A_{\text{pore}}}{A_{\text{tot}}} \tag{2}$$

where, N_{pore} is number of pores on an area A_{tot}, and A_{pore} is the mean pore area.

If H ($= N_{\text{cell}}A_{\text{cell}}/A_{\text{tot}}$) is the hexagonality of the surface with N_{cell} the number of cells on an area A_{tot} and A_{cell} the mean cell area, the porosity can also be written as

$$P = \frac{H\pi}{2\sqrt{3}}\left(\frac{d}{D}\right)^2 \tag{3}$$

Using eqn (3) and (1), the mean wall thickness can be written as

$$w = d\left(\sqrt{\frac{\pi H}{2\sqrt{3}P}} - 1\right) \tag{4}$$

Therefore, from the values of d, P and H evaluated by means of image analysis, w can be calculated. The respective results are listed in Table 1, for a typical $H = 70\%$, with the same uncertainty assigned to w as derived for d. The resulting mean w is in agreement with single values measured across sparse cells, with the additional advantage of providing a statistical validity over all the surface area imaged.

From image analysis of SEM image in Fig. 1, it turns out that the gold-coated APA substrates have a pore diameter of (157 ± 35), (59 ± 9) and (15 ± 3) nm, for the samples shown in Fig. 1(d′), (e′) and (f′), respectively.

SERS measurements were carried out by means of an inVia (Renishaw, New Mills, UK) microspectrometer, with a spectral resolution of 1.10 cm^{-1} with the help of a holographic grating of 1800 grooves mm^{-1}. The samples were excited using the 633 nm laser wavelength (laser power 5.5–55 μW) in backscattering configuration through a 100× objective (NA-0.90) and with an accumulation time of 20 s. The Raman band of the Si wafer at 520 cm^{-1} was used to calibrate the spectrometer. The scattering intensity was collected in the range between 300 and 1700 cm^{-1}. Spectral data were analyzed using Renishaw WiRE software 3.0.

Electric field calculation

With the aim of providing additional information on the Raman behavior of the APA substrates, we have performed numerical simulations of AuAPA structures. In particular, by means of CST Microwave Studio, we have simulated a 25 nm thick layer of gold illuminated by a 633 nm wavelength electromagnetic continuous wave. This analysis, which will be illustrated in detail in the next section, takes advantage of the adaptive tetragonal mesh provided by CST which is capable of describing well the geometrical characteristics of the simulated structure. This aspect plays a crucial role, in particular for structures showing small details in an overall extended domain. In our case, the extension of the three-dimensional domain was of 3.2 μm × 3.8 μm × 25 nm with a resolution of less than 5 nm.

Results and discussion

SEM images of all the APA substrates before and after gold deposition are shown in Fig. 1(d–f) and Fig. 1(d′–f′), respectively. Various fluorescent molecules/proteins were deposited using a chemisorption technique to verify the SERS activity of the AuAPA substrates.

CV (see Fig. 2a for the absorption spectrum and molecular structure) is an organic dye molecule intensively used in biology and medicine as a histological stain. It is an effective stain applied for highlighting acidic components of tissues and is commonly used for nerve tissue sections. SERS measurements were carried out for CV deposited on different APA substrates in the range of 300–1300 cm^{-1}. Raman measurements were also carried out after 2 μl drop-deposition of CV on a flat non-patterned silicon wafer substrate (Fig. 2b). The Raman spectrum of this structure is relatively featureless, with an exponentially increasing fluorescence background and a single characteristic peak of CV at

Table 1 APA substrates specifications, calculated from SEM images by using Igor software grain analysis

	Sample					
	APA1		APA2		APA3	
Parameters	Bare	Au-coated	Bare	Au-coated	Bare	Au-coated
Pore diameter, d/nm	181 ± 45	157 ± 35	82 ± 7	59 ± 9	29 ± 4	15 ± 3
Wall thickness, w/nm	82 ± 35	104 ± 35	21 ± 7	40 ± 9	13 ± 4	36 ± 3
Pore density, $\sigma/10^5$ cm^{-2}	1.7	1.1	9.2	9.4	53	35
Porosity, P (%)	43	15	49	26	35	6

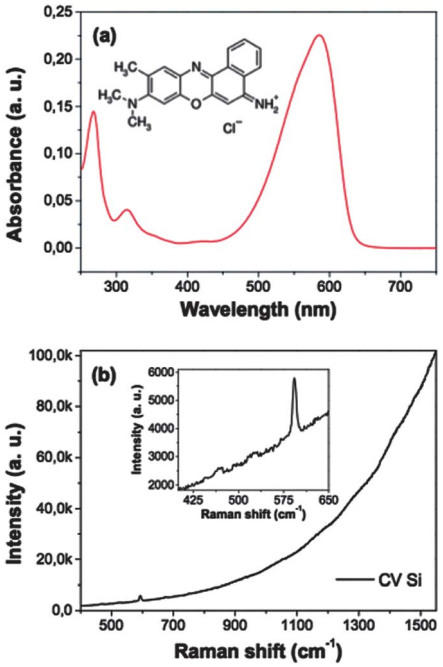

Fig. 2 (a) Optical absorption spectrum of CV with its molecular structure in the inset; (b) Raman spectrum of CV drop cast on the Si substrate ('CVSi') in the range of 400–1550 cm^{-1}. In the inset, the zoomed Raman spectrum in the range of 400–650 cm^{-1} is shown. The fluorescence background is observed in the Raman spectrum of CV.

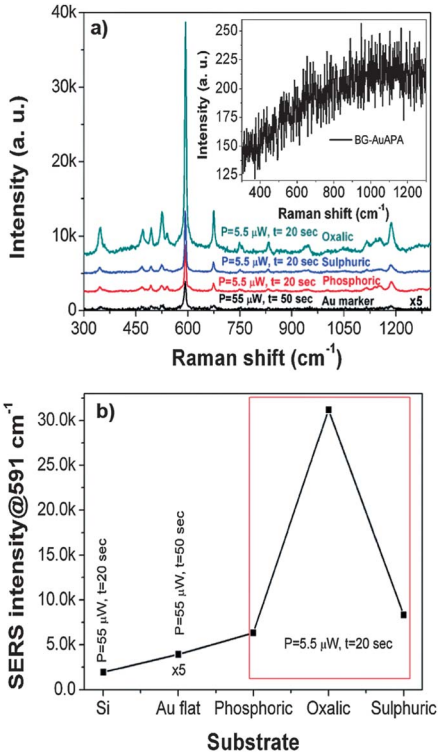

Fig. 3 SERS spectra of CV dye on different AuAPA substrates: (a) SERS spectra of CV (3.46×10^{-6} M) deposited on AuAPA substrates ('CVAuAPA1', 'CVAuAPA2' and 'CVAuAPA3') using a chemisorption technique. Inset of (a): background Raman spectrum of AuAPA substrate; b) reference intensity of 591 cm^{-1} from CV dye, deposited over various substrates, where the measurement parameters are also mentioned. The SERS enhancement factor is estimated to be 0.98×10^3, 1.0×10^4 and 1.12×10^3 for AuAPA1, AuAPA2 and AuAPA3 (100×, NA-0.9), respectively, with respect to the flat gold surface (150×, NA-0.95) with the assumption that the molecules are closely packed.

~591 cm^{-1}. In the inset of Fig. 2b, the zoomed Raman spectrum of CV in the range of 400–650 cm^{-1} is shown.

In Fig. 3a, the SERS spectra of CV on different AuAPA substrates are shown. SERS substrate background measurement (no dye on AuAPA pattern) was carried out and is shown in the inset of Fig. 3a, which shows a flat background response without any Raman band at all. Similar measurements were carried out for all of the three different SERS AuAPA substrates, giving an identical Raman vibrational frequency of CV. The spectra are illustrated in off-set mode for all the SERS substrates for clarity reasons.

In all the SERS spectra of the CV molecule, performed on the AuAPA substrates with different pore diameters (15–160 nm) and wall thicknesses (36–100 nm) (Fig. 3a), the characteristic vibrational bands of CV are observed.[23] Intense Raman bands centred at around 348, 591, 675 and 1186 cm^{-1} can be attributed to the out-of-plane skeleton deformation, combination of in-plane N–H_2 and ring bending, ring deformation and combination of N–H_2 rocking and C–H_x rocking, respectively.[23,24] From the vibrational bands observed in the Fig. 3a it is most probable that the CV is oriented in such a way that the –N–H_2 group is closer to the gold film, leading to the strong Raman scattering and, consequently, higher SERS signal. Additionally, in Fig. 3a, the high exponential background appearing in Fig. 2b for CV deposited over the silicon substrate has disappeared. Hence, significant fluorescence quenching is also illustrated, as already observed in the past for gold nanoparticles.[21]

When the pore size/wall thickness of AuAPA substrate decreases from ~160 nm/~100 nm to ~60 nm/~40 nm, as reported in Table 1, a significant increase in SERS intensity for the CV bands is observed with respect to the flat Au surface/Si substrate, shown in Fig. 3a. The reference band intensity of CV, centred at around 591 cm^{-1}, for different SERS substrates is illustrated in Fig. 3b, in which an increase in intensity from around 2000 counts to more than 30000 counts is observed, while keeping all the measurement parameters fixed but varying the pore size and wall thickness (see Table 1). Furthermore, decrease in d and w leads to decrease in the band intensity. Hence, it is very important to choose the value of d and w with extreme care. To be noted, if we make the hypothesis that the molecules are attached only on the top of the AuAPA walls, then the number of molecules under scan is highest for AuAPA3 (lowest porosity of 6%) and lowest for AuAPA2 (highest porosity of 26%), with an intermediate value for AuAPA1 (porosity of 15%).

From SERS spectra of CV on different gold-coated APA substrates, shown in Fig. 3(a–b), enhancement factor G,

$$G = \left(\frac{I_{\mathrm{SERS}} \Big/ N_{\mathrm{SERS}}}{I_{\mathrm{Raman}} \Big/ N_{\mathrm{Bulk}}} \right)$$

can be evaluated. The enhancement factor varies, depending on the vibration band frequency. In this equation, I_{SERS} is the SERS

intensity of the particular peak of CV whereas I_{Raman} is the normal (not enhanced) Raman intensity of the CV deposited on flat gold surface. N_{SERS} is the number of molecules under laser spot focus contributing to the SERS signal, while N_{Bulk} is the number of molecules contributing to the normal Raman signal. The number of molecules can be calculated using the CV concentration in solution, the porosity of the APA substrate.

Since no other band except 591 cm^{-1} was well observed for the positive control (CVSi substrate, Fig. 2b), this is the only possible band for evaluation of G. Since CV deposition on silicon through chemisorption is not possible because it would not leave any molecule on the silicon substrate after rinsing with water, drop deposition of CV with the concentration of 10^{-3} M was made, and then measurements were carried out on this sample (see Fig. 3a). We, herein, suppose that the molecular size is approximately 20 nm^2 and the molecules are closely packed. However, the enhancement factor G is calculated for AuAPA substrates with respect to the flat gold substrate and is found to be in the range of 0.98×10^3 to 1.0×10^4 in all the three cases, with the highest value of 1.0×10^4 appearing for AuAPA2. This substrate is not the one with smallest pores (and, therefore, also higher pore density) and wall thickness, which is actually AuAPA3. For calculation, only the molecules attached to the AuAPA surface were considered. The molecules attached into pores were not considered in the SERS enhancement factor because the interior part of the pores were out of focus which contribute negligible signal from this area. Here, we propose that the higher enhancement factor G for AuAPA2 with respect to AuAPA1 and AuAPA3 is not solely due to the pore size or wall thickness, but it could be dependent on the combination of them (d and w).

The present results found to be highly reproducible, since SERS spectra of CV taken at different points of each substrate appeared very similar to the respective one, reported in Fig. 3a, which is an intrinsic confirmation of the good uniformity of APA geometry as well as gold coating. In this regard, SERS mapping measurements were also performed in a large area and, thereafter, the analysis was performed for the reference peak centred at 591 cm^{-1}. The statistical analysis such as standard deviation over the whole SERS spectra was also performed for all the substrates. The mapping area, its image analysis and thereafter the SERS spectrum with standard deviation for the AuAPA2 substrate were shown in Fig. 4(a–c) whereas for the other two substrates AuAPA1 and AuAPA3 these are shown in supplementary Fig. S3† (Supplementary Info: section 3). The figures show very small variation in intensity throughout the mapping region. In addition, the comparison between Fig. 2b and Fig. 3b demonstrates that with the APA substrate it is possible to obtain a strongly enhanced Raman signal even for fluorescent molecules. Note that without the APA substrate the fluorescence background covers the whole Raman signal instead.

CV deposited SERS measurements were also performed on a commercially available APA substrate (Fig. S4,† Supplementary Info: section 4). A much lower signal (2700 counts, $t = 20$ s and $P = 0.12$ mW) was found in this case ($AuAPA_{commercial}$) with respect to the AuAPA2 or AuAPA3 substrate prepared in our lab. This can be partly due to the smaller pore diameter, ~20 nm compared to ~200 nm. However, a partial effect may also be due to the better uniformity of the substrates realized in this work (AuAPA1–AuAPA3), which results in a more homogeneous and

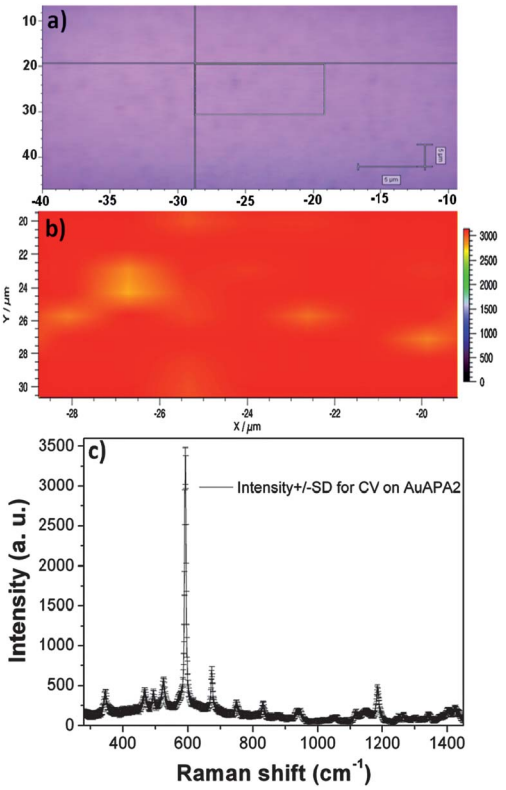

Fig. 4 (a) Optical image of the sample and the crossed area is the place where the mapping was performed ($P = 5.5$ μW, $t = 1$ s); (b) the analysis is performed for the Raman band of CV centred at 591 cm^{-1} and (c) SERS spectrum of CV with the standard deviation for all the spectra in the mapping.

monodisperse pore diameter (±18% for AuAPA1 and ±14% in the case of AuAPA2) (see Table 1) as compared to the commercial $AuAPA_{comm}$ (<30% which will be 125 ± 50 nm). Fabrication of the commercial APA is probably based on hard anodization with a high electric field and high ionic current, which provides a faster growth at the expense of the pore size homogeneity and pattern uniformity.

In order to provide support for the experimental results shown in Fig. 3, we have also performed a series of simulations with the intent of calculating the near field electromagnetic distribution on the APA substrates. This kind of analysis can, in fact, provide information on the level of excitation of any sample deposited on a SERS substrate. In Fig. 5, simulations of the electric field due to the LSP generation on SERS substrates at $z = 0$ nm (*i.e.* on the front surface of the substrate) using CST software are presented. In particular, a 25 nm thick golden slab showing a honeycomb pattern with a varying periodicity of 260, 100 and 55 nm, and sub-wavelength air holes[25] with a diameter of 160, 60 and 15 nm, respectively, was simulated. The source light was taken at 633 nm with linear polarization along the x-axis. The overall simulated structure is shown in Fig. 5a. For all the periodicity patterns, the results show an electric field strongly affected by the material discontinuity. In fact, the absolute value of the total electric field shows some nodes at the gold–air interface. This is justified by the z-component of the electric field as in Fig. 5b. The x-polarization creates anti-phase hot spots along the x-axis which

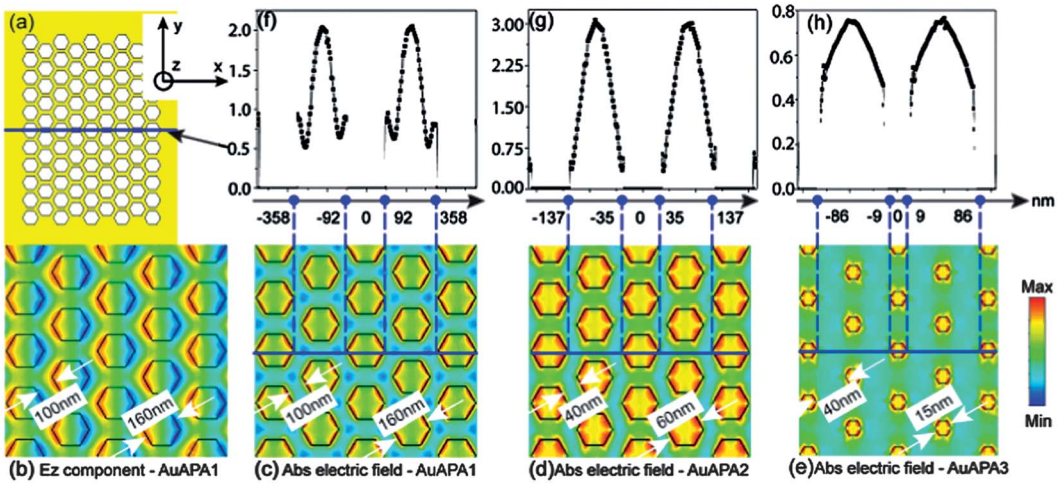

Fig. 5 CST simulations of honeycomb structures by varying pore size d and wall thickness w ($=D-d$): (a) the overall simulated structure; (b) amplitude of the z-component of the electric field in the x–y plane of AuAPA1; total electric field in the x–y plane for (c) AuAPA1 with $d = 160$ nm and $w = 80$ nm, (d) AuAPA2 with $d = 60$ nm and $w = 40$ nm, (e) AuAPA3 with $d = 15$ nm and $w = 40$ nm; (f), (g) and (h) relative electric field profile over the gold surface along the highlighted line for all the SERS structures. The excitation light is $\lambda = 633$ nm on the SERS surface with the dielectric function of the gold slab $\varepsilon_{real} = -9.83$ and $\varepsilon_{imaginary} = 1.97$. The gold thickness is always $h = 25$ nm.[26]

determines the abrupt change of the electric field as in Fig. 5(c–e). The red color in the electric field distribution is the maximum while the blue color is for the minimum. The relative electric field distribution profile over the gold surface area for all AuAPA substrates with respect to the AuAPA3 substrate are shown in Fig. 5(f–h). It is easily understood that the intensity of the field is proportional to the coupling strength between the holes. This coupling decreases when the holes are far from one another. This aspect is especially stressed when we look at the relative value of electric field for all the samples. In this case AuAPA2 shows a value which is 10 times higher than the AuAPA3 substrate. These simulation findings were found in good agreement with the experimental results shown in Fig. 3.

To understand the 3-dimensional device morphology, one can further take advantage of the AFM analysis. In Fig. 1(b–c), it can be observed in the AFM image that the gold evaporation forms a grainy layer on the top of APA pore wall edge. Furthermore, the adsorption of the dye molecules can occur only on the gold surface.

From both the experimental measurements of CV molecules deposited on the different APA substrates (Fig. 3) and the respective simulations (Fig. 5), we found that the substrate providing the best enhancement is 'AuAPA2'. The total enhancement of Raman intensity in the SERS phenomena is a combination of factors such as an increase in electric field (due to the metal surface nano-structure size, shape, and inter-particle gap) and of an increase of the molecular polarizability (*i.e.* chemical enhancement). It is found that the major part of the signal enhancement is due to the electric field enhancement, whereas the maximum chemical enhancement could be about 100.[27] To confirm and better clarify the observed high enhancement, we performed further investigations with the different selected biomolecules (Rd6G and GFPmut2) on the AuAPA2 substrate.

Rd6G is a dye molecule, used in biotechnology applications such as fluorescence microscopy. It is also used as a laser dye in dye lasers. The molecular structure and the absorption spectrum are shown in Fig. 6a. SERS measurements were performed for the Rd6G dye sample, deposited over 'AuAPA1' and 'AuAPA2' SERS substrates, in the range of 700–1800 cm^{-1} (see Fig. 6b). Well defined SERS spectra are observed for the substance deposited over the 'AuAPA' substrate. Various characteristic peaks of Rd6G at around 775, 1182, 1310, 1361, 1510 and 1649 cm^{-1} are observed, which can be attributed to the out-of-plane C–H_x bending, a combination of C–H and N–H bending, a combination of ring stretching of C–C vibration, N–H bending and C–H_x wagging, C–H bending, a combination of C–N stretching, C–H and N–H bending, and a combination of ring stretching of the C–C vibration and C–H_x bending, respectively.[8,28,29] In addition, one shoulder at around 1275 cm^{-1} was also observed, which could be attributed to the C–O–C stretching vibration of the xanthene moiety.

In the past, resonance Raman spectroscopy and enhanced Raman spectroscopy (in case of Rd6G adsorbed to a silver surface) have been reported[29–31] for the Rd6G molecule. However, a small Raman shift could be found when observing the SERS and resonance Raman spectra, and the results of these two techniques appear very similar except for the change in peak ratio of these bands (1361, 1510, and 1649 cm^{-1}). The variation in peak intensity ratio is, certainly, due to the fact that with a different metal surface the molecule tends to adsorb differently. The molecule adsorption depends on the electronegativity of the metal (higher for Au than for Ag). It can be observed in the results presented in ref. 31 that the SERS spectrum of Rd6G attached to the Ag surface shows the highest peak centred at 1649 cm^{-1}, whereas in case of Rd6G attached to the Au surface the two peaks at around 1361 and 1510 cm^{-1} are the most intense features. As per the SERS selection rule, the strong intensity of in-plane vibrational modes (1361 and 1510 cm^{-1} in case of the Au surface and 1649 cm^{-1} for the Ag surface bound molecule) in the SERS of Rd6G suggests the perpendicular orientation of the molecules to the metal surface.

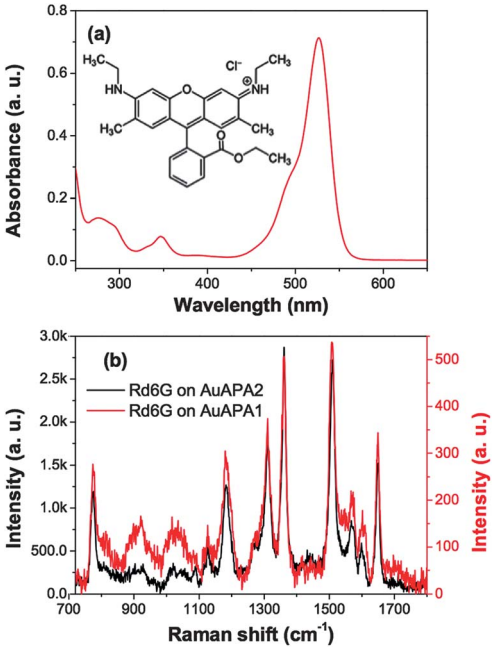

Fig. 6 (a) Optical absorption spectrum of Rd6G with its molecular structure in the inset; (b) SERS spectra of Rd6G in the range of 700–1800 cm^{-1}. The power is ~8 μW and the accumulation time is 20 s.

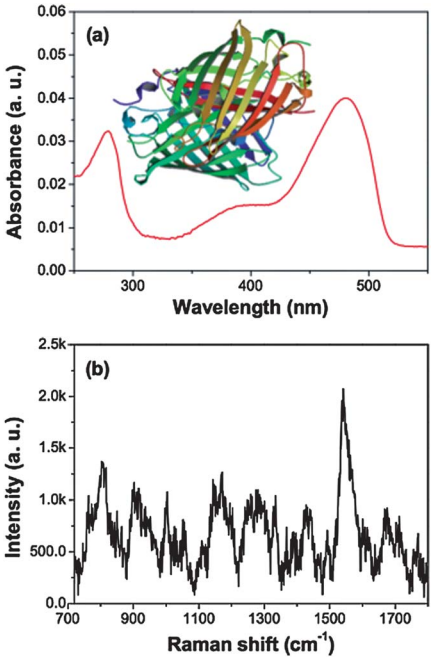

Fig. 7 (a) Optical absorption spectrum of GFPmut2 with its molecular structure in the inset; (b) SERS spectrum of GFP in the range of 700–1800 cm^{-1}, deposited over the AuAPA2 substrate. The power is kept at 0.4 mW and the accumulation time is fixed to 30 s.

Green fluorescence protein (GFP) is a fluorescent protein, composed of 238 amino acids (around 27 kDa). It exhibits green fluorescence when it is excited by a blue light. GFPmut2 is a triple mutation of GFP (S65A, V68L, and S72A).[30] The importance of this fluorescence protein is that GFP has highly efficient fluorescence recovery and has a very sharp irradiation wavelength, which makes it highly useful for intracellular studies of slow biological processes by means of single-molecule two-photon excitation processes.[33] The ribbon molecular structure of GFPmut2 and its absorption spectrum are shown in Fig. 7a.

The SERS spectrum of the GFPmut2, deposited over the AuAPA3 SERS substrate, is illustrated in Fig. 7b in the range of 850–1800 cm^{-1}. Various sharp bands are observed at around 1000, 1368 and 1500 cm^{-1}, which are related to the ring stretching of the phenylalanine amino acid, C–C stretching of aliphatic groups and C–C stretching of the tryptophan and phenylalanine groups, respectively. Additionally, various broad bands were also present that can be assigned to C–H_x rocking (1100–1200 cm^{-1}), C–O stretching (1250 cm^{-1}), C–H_x bending and C–N stretching (1400–1450 cm^{-1}), C=N stretching (1500–1540 cm^{-1}) and C=O stretching at around 1675 cm^{-1}. Recently, femtosecond Raman scattering (FSRS) measurements were performed on GFP to investigate the protonation/deprotonation upon irradiation.[34] There are many similarities in our results with the results presented by Fang *et al.*, except for a few peaks (*e.g.* 1003 cm^{-1}), which are more pronounced in our case because of the excitation wavelength of 633 nm.

Conclusions

Various home-built AuAPA substrates with varying pore size and wall thickness were utilized for large-area SERS substrates. Various organic molecules (CV and Rd6G dyes, and GFPmut2 protein) were deposited using a chemisorption technique, through which a monolayer of molecules can be achieved. It is observed that the AuAPA2 substrate ($d = 59 \pm 9$, $w = 40 \pm 9$) demonstrates the maximum signal enhancement G. CST simulations of the electric field distribution on these ordered and reproducible SERS substrates were also performed, keeping the structural parameters as close as possible to the experimental honey-comb nanostructures. Theoretical results follow the same trend of experimental findings. The major advantage of using nanoporous alumina substrates, as compared to the traditional colloidal coating or lithographic processing, is a good trade-off between the high enhancement factor G obtained and the large surface area produced. The surface of the present samples is of the order of 1 cm^2 but it can be easily increased in multiple folds. Comparison between commercial and home-built APA templates found that the latter appear better SERS substrates. The respective SERS enhancement factor G is estimated to be ~4 × 10^6. Additionally, the sensing efficacy of the fabricated SERS devices on different dyes and proteins (CV, Rd6G and GFP in our case) opens the way for real application as a biosensor. Further research should be made in order to optimize G on the basis of the substrate parameters of pore size, wall thickness, and thickness of the gold coating. The easy and inexpensive processing required for APA SERS fabrication would also make these substrates disposable, opening the way to their large-scale applications.

Acknowledgements

Mr. Mario Malerba and Dr. Sergio Marras from the Electron Microscopy laboratory of the IIT Nanochemistry Department

are gratefully acknowledged for their assistance in SEM imaging and related sample preparation. G. Das, R.P. Zaccaria, A. Toma, A. Diaspro and E. Di Fabrizio acknowledge the European project SMD FP7-NMP 2800-SMALL-2 proposal No. CP-FP 229375-2 and NANOANTENNA FP7-HEALTH-2009 grant No. 241818.

References

1 M. J. Ayora Cañada, A. R. Medina, J. Frank and B. Lendl, *Analyst*, 2002, **127**, 1365.
2 K. Kneipp, H. Kneipp and J. Kneipp, *Acc. Chem. Res.*, 2006, **39**, 443.
3 B. Sägmüller, B. Schwarze, G. Brehm and S. Schneider, *Analyst*, 2001, **126**, 2066.
4 B. N. J. Persson, K. Zhao and Z. Zhang, *Phys. Rev. Lett.*, 2006, **96**, 207401–1.
5 C. L. Haynes, A. D. McFarland and R. P. Van Duyne, *Anal. Chem.*, 2005, **77**, 338A.
6 U. Kreibig and M. Vollmer, *Optical Properties of Metal Clusters*, Springer Series in Material Science, Springer, Berlin, 1995.
7 X. Hou and Y. Fang, *J. Colloid Interface Sci.*, 2007, **316**, 19.
8 M. L. Coluccio, G. Das, F. Mecarini, F. Gentile, A. Pujia, L. Bava, R. Tallerico, P. Candeloro, C. Liberale, F. De Angelis and E. Di Fabrizio, *Microelectron. Eng.*, 2009, **86**, 1085.
9 E. C. Le Ru, J. EtchegoinGrand, N. Felidj, J. Aubard, G. Levi, A. Hohenau and J. R. Krenn, *Curr. Appl. Phys.*, 2008, **8**, 467.
10 G. Das, F. Mecarini, F. Gentile, F. De Angelis, M. H. G. Kumar, P. Candeloro, C. Liberale, G. Cuda and E. Di Fabrizio, *Biosens. Bioelectron.*, 2009, **24**, 1693.
11 M. Salerno and R. Cingolani, *J. Micromech. Microeng.*, 2007, **17**, 2414.
12 X. Zhang, A. V. Whitney, J. Zhao, E. M. Hicks and R. Van Duyne, *J. Nanosci. Nanotechnol.*, 2006, **6**, 1.
13 P. N. Barlette, J. J. Baumberg, P. R. Birkin, M. A. Ghanem and M. C. Netti, *Chem. Mater.*, 2002, **14**, 2199.
14 C. L. Haynes and R. Van Duyne, *J. Phys. Chem. B*, 2001, **105**, 5599.
15 X. Y. Ling, C. Acikgoz, I. Y. Pang, M. Hempenius, D. N. Reinhoudt, G. J. Vancso and J. Huskens, *Nanoscale*, 2010, **2**, 1455.
16 R. P. Zaccaria, P. Verma, S. Kawaguchi, S. Shoji and S. Kawata, *Opt. Express*, 2008, **16**, 14812.
17 R. P. Zaccaria, S. Shoji, H. B. Sun and S. Kawat, *Appl. Phys. B: Lasers Opt.*, 2008, **93**, 251.
18 L. Zhang, H. S. Cho, F. Li, R. M. Metzger and W. D. Doyle, *J. Mater. Sci. Lett.*, 1998, **17**, 291.
19 Y. Li, Z. Y. Ling, S. S. Chen and J. C. Wang, *Nanotechnology*, 2008, **19**, 225604.
20 R. Zhang, K. Jiang and G. Ding, *Thin Solid Films*, 2010, **518**, 3797.
21 E. Dulkeith, A. C. Morteani, T. Niedereichholz, T. A. Klar and J. Feldmann, *Phys. Rev. Lett.*, 2002, **89**, 203002.
22 M. Salerno, N. Patra and R. Cingolani, *Nanoscale Res. Lett.*, 2009, **4**, 865.
23 E. Vogel, A. Gbureck and W. Kiefer, *J. Mol. Struct.*, 2000, **550–551**, 177.
24 A. Kudelski, *Chem. Phys. Lett.*, 2005, **414**, 271.
25 H. J. Lezec and T. Thio, *Opt. Express*, 2004, **12**, 3629.
26 A. D. Rakic, A. B. Djurisic, J. M. Elazar and M. L. Majewski, *Appl. Opt.*, 1998, **37**, 5271.
27 Y. Liu, *Langmuir*, 2002, **18**, 174.
28 B. Mondal and S. K. Saha, *Chem. Phys. Lett.*, 2010, **497**, 89.
29 L. Jensen and G. C. Schatz, *J. Phys. Chem. A*, 2006, **110**, 5973.
30 B. Dong, L. Liu, H. Xu and M. Sun, *J. Raman Spectrosc.*, 2010, **41**, 719.
31 H. Watanabe, N. Hayazawa, Y. Inouye and S. Kawata, *J. Phys. Chem. B*, 2005, **109**, 5012.
32 B. P. Cormack, R. H. Valdivia and S. Falkow, *Gene*, 1996, **173**, 33.
33 G. Chirico, A. Diaspro, F. Cannone, M. Collini, S. Bologna, V. Pellegrini and F. Beltram, *ChemPhysChem*, 2005, **6**, 328.
34 C. Fang, R. R. Frontiera, R. Tran and R. A. Mathies, *Nature*, 2009, **462**, 200.

